Available online at www.sciencedirect.com
ScienceDirect
International Journal of Heat and Mass Transfer 51 (2008) 526–538
International Journal of HEAT and MASS TRANSFER
www.elsevier.com/locate/ijhmt

Comparative study of heat transfer and wetting behaviour of conventional and bioquenchants for industrial heat treatment

Peter Fernandes, K. Narayan Prabhu *

Department of Metallurgical and Materials Engineering, National Institute of Technology Karnataka, Surathkal, P.O. Srinivasnagar 575 025 Mangalore, Karnataka State, India

Received 5 February 2007; received in revised form 9 May 2007
Available online 30 July 2007

Abstract

An investigation was conducted to study the suitability of vegetable oils as bioquenchants for industrial heat treatment. The study involved the assessment of the severity of quenching and wetting behaviour of conventional and vegetable oil quench media. Quench severities of sunflower, coconut and palm oils were found to be greater than mineral oil. The quench severity of aqueous media is greater than oil media although their wettability is poor as indicated by their higher contact angles. A dimensionless contact angle parameter defined in this work is found to be a better parameter to compare the wetting behaviour with heat transfer.

Keywords: Quench severity; Heat transfer; Wetting; Contact angle; Bioquenchants

1. Introduction

Quenching of steels involves the process of heating a part to austenitizing temperature and holding at this temperature for a specified time followed by intense cooling in a suitable quench medium. Quenching prevents the formation of ferrite or pearlite and allows the formation of bainite or martensite. The effectiveness of quenching depends on the cooling characteristics of the quenching medium and the ability of steel to harden. Achieving desired hardness, strength or toughness and minimizing the possibility of occurrence of quench cracks due to evolution of residual stresses are the key indicators of successful hardening process [1,2].

The severity of quenching or the cooling power of a quench medium is estimated by measuring the thermal response of a heated probe brought in contact with it. It is a measure of the ability of a quenchant to extract heat from a sample during quenching. Cooling curve analysis method is most useful for assessing the cooling characteristics of a quenching medium [3,4]. The cooling curve of the quench probe provides continuous cooling information throughout the three stages of quenching process, namely, vapour phase, nucleate boiling and convective cooling [5]. Lumped heat capacitance method, Kobasko's method and Grossman's hardenability method are some of the techniques available for the assessment of severity of quench medium. These methods are used purely for assessment of cooling characteristics of quench medium.

Heat removal from the metal during quenching can be quantified in terms of an interfacial heat transfer coefficient (h) or interfacial heat flux (q). The interfacial heat transfer coefficient is defined as the ratio of the interfacial heat flux (q) to the temperature drop (ΔT) at the metal/quenchant interface. A quenchant must impart a sufficiently high interfacial heat flux to produce high cooling rate. The inverse modeling of heat conduction enables the determination of boundary heat flux transients and the specimen surface temperatures. The metal/quenchant interfacial heat transfer data is useful in simulation based quench process design that would enable the heat treater to judiciously select the quench medium for specific applications.

* Corresponding author. Tel.: +91 824 2474000x3756; fax: +91 824 2492794.
E-mail address: prabhukn_2002@yahoo.co.in (K.N. Prabhu).

0017-9310/$ - see front matter © 2007 Elsevier Ltd. All rights reserved.
doi:10.1016/j.ijheatmasstransfer.2007.05.018

Nomenclature

A	surface area of the probe (m^2)
Bi	generalized Biot number
C	specific heat of the probe material (J/kg K)
h	heat transfer coefficient (W/m K)
$\bar{h}$	mean heat transfer coefficient (W/m K)
H	Grossman hardenability factor (m^{-1})
k	thermal conductivity of the probe material (J/kg K)
K	Kondratjev form factor
q	heat flux density (W/m^2)
R	mean surface roughness (m)
t	time (s)
T	temperature of the quenchant (°C)
V	volume of the probe (m^3)
TAN	total acid number
IN	iodine number

Greek symbols

α	thermal diffusivity (m^2/s)
ϕ	dimensionless contact angle
γ	surface energy (J/m^2)
ν	kinematic viscosity (m^2/s)
θ	contact angle (°)
ρ	specific density of the probe material (kg/m^3)
τ	dimensionless time

Subscripts

a	average roughness
i	initial condition
k	Kobosko coefficient
ls	liquid–solid interface
lv	liquid–vapour interface
n	character for use with Kondratjev number
p	probe material
m	quench medium
r	reference condition
v	character for use with generalized Biot number
sv	solid–vapour interface

The rate of heat removal from a heated component by a quenchant also depends on the ability of the liquid medium to wet and spread on its surface [6]. Wettability can be characterized by the degree and the rate of wetting [7,8]. The degree of wetting indicates the extent up to which the liquid wets the surface and generally quantified in terms of contact angle formed at the three-phase interface. Under equilibrium conditions it is dependent on the surface and interfacial energies involved at the solid–liquid interface. The rate of wetting indicates how fast the liquid spreads on the surface. It is governed by number of factors like thermal conditions, viscosity of liquid, surface conditions, etc. The basic mathematical treatment of wetting of a solid surface by liquid is given by Young–Dupre equation:

$$\cos\theta = (\gamma_{sv} - \gamma_{sl})/\gamma_{lv} \quad (1)$$

The above equation assumes equilibrium of interfacial energies and also gives an expression for equilibrium contact angle (θ) formed at the three-phase contact point [9,10]. For practical purposes, the liquid is said to wet the surface of solid when the contact angle is less than 90°. On the other hand, if the contact angle is greater than 90°, the liquid is considered as non-wetting the solid. In such cases, the liquid drop spreads easily on the substrate surface and do not have any tendency to enter into pores or holes by capillary action. It is expected that heat transfer and wetting characteristics of the quench medium are closely related. Improved wetting will enhance the rate of heat transfer from solid to liquid.

Petroleum based oils are generally used as quenchants for industrial heat treatment. But petroleum based products are non-renewable and can contribute to air and water pollution. The need to achieve energy independence and high cost of the crude petroleum is directing so much focus on vegetable oils and crops that will help to yield these oils. The use of vegetable oils as quench media (bioquenchants) has many advantages for industrial heat treatment. Bioquenchants are safer for the environment because these are available from natural materials that are renewable and readily biodegradable [11,12].

The present investigation is carried out to explore the suitability of vegetable oils as bioquenchants for industrial heat treatment of commercial steels. This would have immense benefits from the environmental and economical point of view. The determination of quench severity and quantification of the boundary conditions at the metal/quenchant interface would be of considerable utility to the heat treating community. There are several methods of assessment of severity of quenching and heat transfer from the probe to the quench medium. It is essential to compare the various techniques to obtain a meaningful estimate of the cooling power of the quench medium. This data would be useful to assess the possibility of replacing petroleum based quench media by vegetable oil quenchants. Further, the wetting behaviour of bioquenchants and its interaction with heat transfer phenomenon is not yet investigated. Hence the present work is carried out with the following objectives:

(i) Evaluation of the various methods of assessment of severity of quenching of bioquenchants.
(ii) Estimation and comparison of quench severity of bioquenchants with conventional quench media.

(iii) Assessment of wetting behaviour of quench media and investigation of interaction between wetting and cooling kinetics of the quench medium.

2. Experimental

The experimental set-up for estimation of quench severity consists of a vertical tubular electric resistance furnace open at both ends. A beaker containing 2000 ml of quenchant was placed directly underneath the furnace so that the heated probe could be transferred quickly to the quenching medium. Water, 5% brine and a mineral oil (SN150) were selected as quench media. Apart from these conventional quenchants, five vegetable oils namely, coconut, sunflower, palm, castor and groundnut oils were used. Quench probes for end and lateral quenching were prepared from Type 304 stainless steels and used for assessment of severity of quench and assessment of metal/quenchant interfacial heat transfer. Stainless steel (Type 304) material was selected over carbon steels to avoid the effect of phase transformation on heat transfer. The lateral quench probe had a diameter of 12 mm and height 60 mm. The height to diameter ratio for this quench probe was 5 and this ensures heat transfer in the radial direction. However, for the end quench probe the diameter and height were 25 mm and 50 mm, respectively. Inverse analysis technique was adopted for the end quench probe for estimation of heat flux transients. All the probes were instrumented with K-type thermocouples of 0.45 mm diameter. The dimensions of the probes and locations of the thermocouples (TC/TC1/TC2) are given in Fig. 1a and b, respectively. All the thermocouples were connected by means of compensating cables to a data-logger interfaced with the computer. The probe was heated to 850 °C in an electric resistance furnace and held vertically inside the furnace using a nichrome wire for 5 min and was transferred to a beaker containing 2000 ml of the quenchant placed directly beneath the furnace. The transfer of the probe to the quench bath was done manually using the nichrome wire wound over a pulley attached to the top of the furnace. The process of transfer of the probe to the quench bath took less than 3 s.

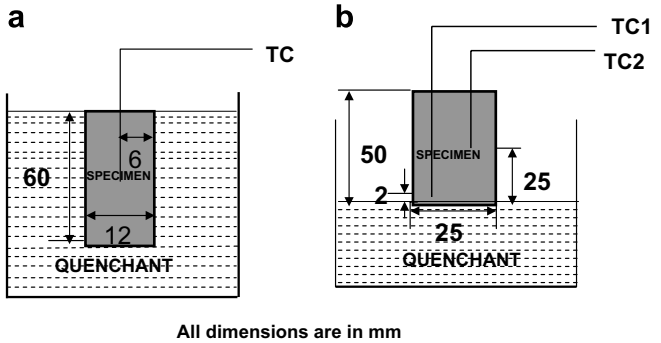

Fig. 1. Schematic sketches of (a) lateral quenching set-up and (b) end quenching set-up.

The following sets of experiments were carried out:

1. Lateral quenching of Type 304 stainless steel probe to assess the severity of quenching.
2. End quenching of Type 304 stainless steel probe and AISI 1040 steel to estimate the surface heat flux transients.

The experimental set-up for wetting studies consists of a dynamic contact angle analyzer (Model: FTA 200 – First Ten Ångstroms, Virginia, USA) which is capable of capturing and analyzing the spreading process of a liquid on a solid. The equipment has a flexible video system for measuring contact angle, surface and interfacial energies. Six oils (mineral, palm, coconut, groundnut, castor and sunflower) along with 5% brine and water were used as test liquids for wetting studies on stainless steel substrates in the temperature range of 30–175 °C. A droplet of test liquid was dispensed by the nozzle onto the steel substrate and spreading phenomena was recorded at 60 frames/s. Captured images were analyzed using FTA software to determine the wetting parameters.

Physical properties of the test liquids like kinematic viscosity, total acid value and iodine value were also determined experimentally. Viscosity of the oil was measured using a Saybolt Viscometer. The total acid number (TAN) and iodine number (IN) were experimentally determined by a procedure as outlined in IS: 548 Part I-1964.

3. Assessment of quench severity – theoretical background

3.1. Grossman hardenability factor (H)

The Grossman quench severity (H) factor is calculated from cooling curve analysis during quenching. Temperature–time curves at the centre of the probe were generated for various values of mean heat transfer coefficients varying from 100 to 3000 W/m^2 K by solving the one dimensional Fourier heat conduction directly using explicit finite difference method. The probes used for simulation and experimental processes are of same dimensions. Fig. 2 shows the cooling curves estimated for varying values of heat transfer coefficient. The peak cooling rates are determined from the simulated cooling curves. The peak cooling rates are plotted as a function of heat transfer coefficient as shown in Fig. 3. The plot is used for estimating the mean heat transfer coefficient from the experimentally determined cooling rates. The Grossman hardenability factor (H) was then calculated as

$$H = \overline{h}/2k \tag{2}$$

3.2. Kobasko's method

Heat transfer coefficient (h_k) can be calculated from the correlation between Kondratjev number (K_n) and generalized Biot number (Bi_v) [13]. The cooling rate (C.R.) found

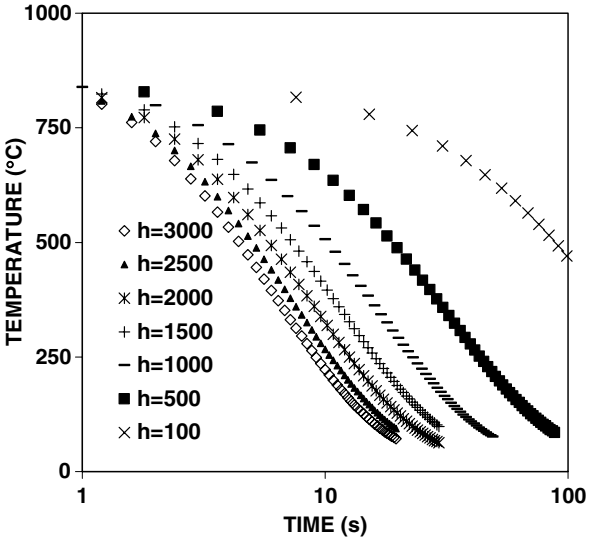

Fig. 2. Effect of heat transfer coefficient on cooling curves.

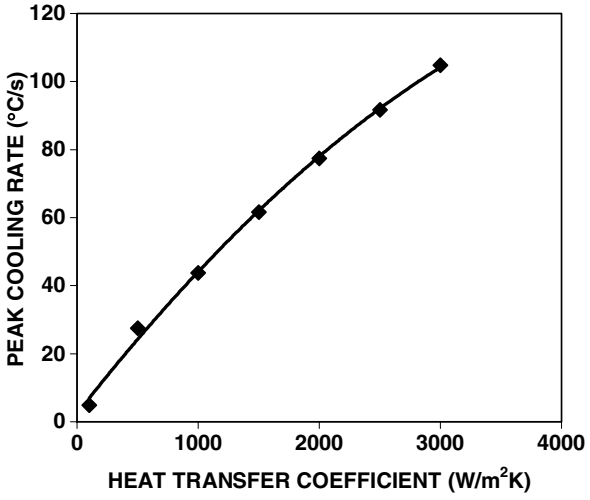

Fig. 3. Peak cooling rate vs mean heat transfer coefficient.

from two points on the cooling curve corresponding to time t_1 and t_2 as

$$\text{C.R.} = \frac{\ln(T_1 - T_q) - \ln(T_2 - T_q)}{t_2 - t_1} \tag{3}$$

where T_q is the temperature of quenchant, K; T_1 and T_2 are temperatures of the probe at time t_1 and t_2, respectively, K.

From the value of C.R., the Kondratjev number (K_n) is calculated as

$$K_n = \text{C.R.}\frac{K}{\alpha} \tag{4}$$

For a cylindrical specimen, $K = \frac{R^2}{5.783}$.

The correlation between K_n and the generalized Biot number (Bi_v) is

$$K_n = \frac{Bi_v}{(Bi_v^2 + 1.437Bi_v + 1)^{1/2}} \tag{5}$$

The heat transfer coefficient (h_k) is calculated from the generalized Biot number as

$$h_k = \frac{Bi_v kV}{KA} \tag{6}$$

Kobosko's technique can be adopted for probes having different sizes.

3.3. Inverse analysis

The advantage of using inverse method is that only the temperature data measured at some proper interior locations of the work-piece are used to calculate surface heat flux transients. The information on exterior conditions such as the properties of cooling media, which are essential in the direct approach, was not required in the inverse method [14–16]. Due to intense heat transfer, significant temperature gradients are achieved close to the quenched surface, which is advantageous for the result of the inverse solution [17,18]. Beck [19] developed a non-linear estimation technique to analyze the transient heat transfer at the metal/quenchant interface. The one dimensional Fourier heat conduction equation in cylindrical coordinates given below,

$$\rho C\frac{\partial T}{\partial t} = \frac{k}{r}\frac{\partial}{\partial r}\left(r\frac{\partial T}{\partial r}\right) \tag{7}$$

was solved inversely. In this inverse technique, the surface heat flux density is estimated from the knowledge of measured temperatures inside a heat conducting solid. This is done by minimizing function:

$$F(q) = \sum_{i=1}^{M_s}(T_{n+1} - Y_{n+1})^2 \tag{8}$$

where s is a small integer and $M = \frac{\Delta\Theta}{\Delta t}$ at regular finite difference intervals. T_n is the calculated temperature and Y_n is the measured temperature at a location close to metal/quenchant interface (TC1). The problem is to find the value of q, which minimizes the sum of the square deviation of the experimentally measured temperatures at TC1 from the estimated temperatures at the same location. $\Delta\Theta$ and Δt are the time steps for the estimation of heat flux and temperature, respectively. Applying the condition $\frac{\partial F}{\partial q} = 0$ on Eq. (3.10) for minimization, the correction for the heat flux (Δq) at each iteration step is estimated. This procedure is continued until the ratio $\left(\frac{\Delta q}{q}\right)$ becomes less than 0.005. This procedure simultaneously yields the temperature of the specimen surface in contact with the quench medium and the interfacial heat flux. The mathematical details of the inverse method as applied to quenching are given in Ref. [20].

4. Results and discussion

4.1. Severity of quench media

Fig. 4 shows the cooling curve and cooling rates at the centre of the Type 304 stainless steel probe subjected to lateral quenching in 5% brine and castor oil.

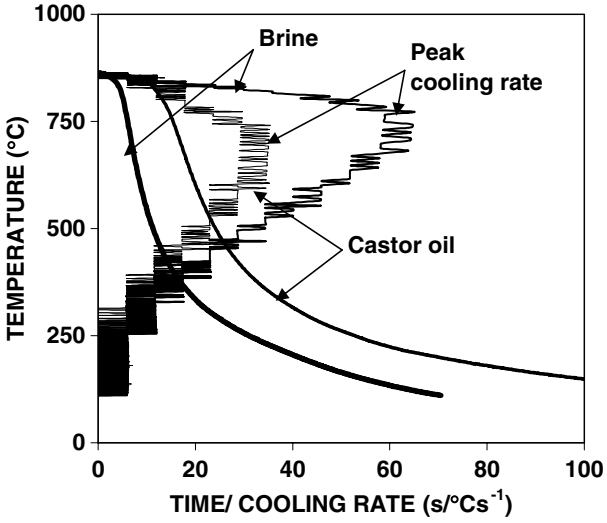

Fig. 4. Typical cooling rate curve of 5% brine and castor oil during immersion quenching of stainless steel probe.

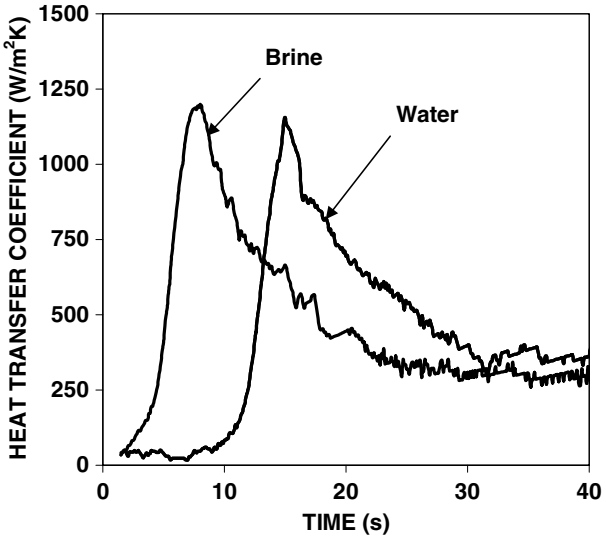

Fig. 6. Variation of heat transfer coefficients (h_k) with time during immersion quenching of stainless steel probe in aqueous media.

4.1.1. Grossman quench severity factor

The Grossman quench severity (H) was estimated to assess the quench severity of quench media. Fig. 5 shows the H factors obtained with different quench media. Higher H factor values were obtained for aqueous media. Among oils, castor oil shows the lowest (11.81 m^{-1}) H factor. Both sunflower and coconut oils yielded similar value of H (21.65 m^{-1}). Conventional mineral oil (18.50 m^{-1}) yielded lower H factor than palm oil (20.47 m^{-1}). Grossman's method was not able to distinguish quench media having nearly the same magnitude of severity of quenching.

4.1.2. Kobasko's method

The variation of heat transfer coefficient (h_k) with time during lateral quenching of stainless steel probe (Type 304) in various quench media are shown in Figs. 6–8. Maximum peak heat transfer coefficient of 1255 W/m^2 K was obtained for 5% brine and minimum peak heat transfer coefficient of 528 W/m^2 K was obtained for castor oil. The peak heat transfer coefficients were obtained during nucleate boiling stage for all the quench media. The enhanced convective transfer of quenchant at the onset of nucleate boiling stage causes a sudden rise in the rate of cooling resulting in higher heat transfer. The cooling rate and heat transfer coefficient were found to be strongly dependent on the viscosity of quench oil. A lower heat transfer rate was observed with higher viscosity oils. Higher viscosity castor oil shows the lowest peak heat transfer coefficient as compared to other oil media whereas lower viscosity sunflower (721 W/m^2 K) and coconut oils (708 W/m^2 K) show maximum peak heat transfer coefficients. The peak heat transfer coefficient of palm oil

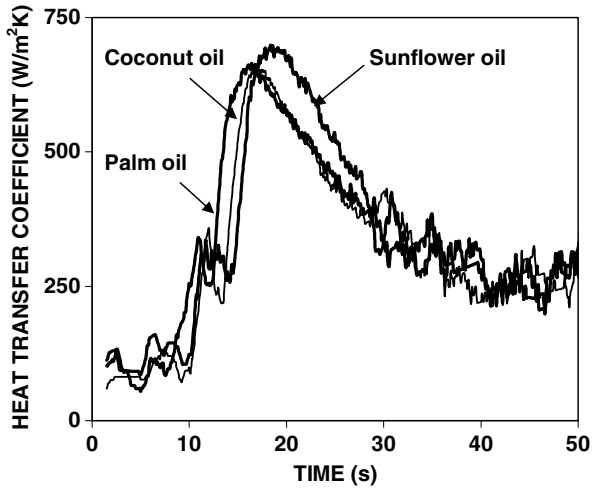

Fig. 7. Variation of heat transfer coefficients (h_k) with time during immersion quenching of stainless steel probe in oil media.

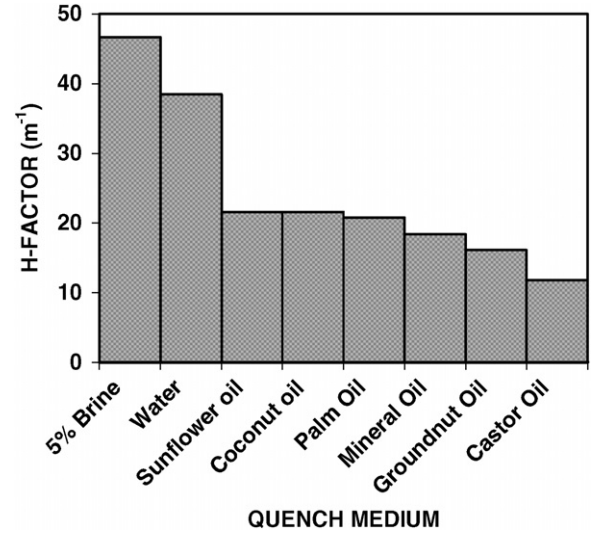

Fig. 5. Grossman H factors estimated for various quench media.

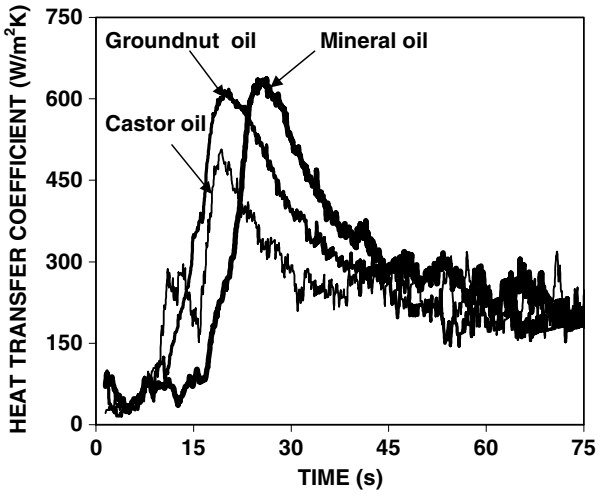

Fig. 8. Variation of heat transfer coefficients (h_k) with time during immersion quenching of stainless steel probe in various oils.

(691 W/m^2 K) was higher than conventional mineral oil (672 W/m^2 K).

4.1.3. Inverse analysis

The variation of heat flux transients with surface temperature during end quenching of stainless steel probe (Type 304) in various quench media is shown in Fig. 9. The heat flux values were low in the initial period of quenching due to the insulating effect of the vapour blanket for all the quench media. The duration of the existence of vapour blanket stage was more for oil media as compared with the aqueous media. The nucleate boiling stage was delayed in oil quenchants compared with aqueous quench media. Heat flux attained its maximum value during the beginning of nucleate boiling stage for all quench media. Peak heat fluxes were obtained in 5% brine and castor oil at about 14.7 and 24.6 s, respectively. During boiling, the

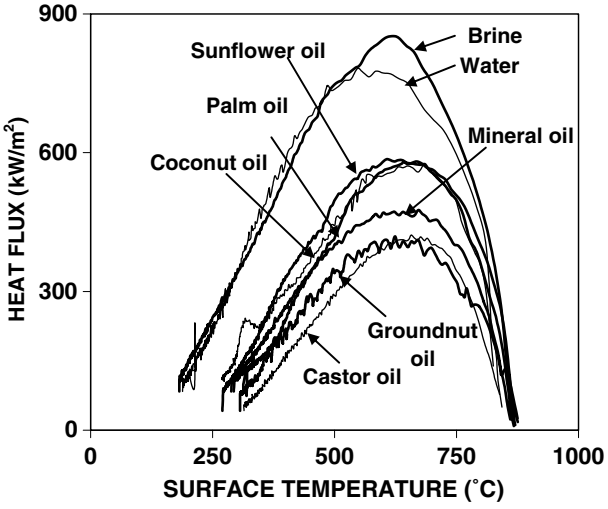

Fig. 9. Variation of heat flux transients with surface temperature during end quenching of stainless steel probe in various quench media.

nucleation of bubbles begins to form at the surface. The bubble growth occurs as a result of evaporation of liquid all around the bubble interface. The energy required for evaporation is supplied by superheated liquid layer that surrounds the bubble. Most of the evaporation occurs at the base of the bubble and the interface [21]. Photographs of stainless steel probe during quenching in palm oil are shown in Fig. 10. Fig. 10a and b shows the formation of a vapour blanket over the entire surface of the probe. The transition of vapour blanket phase to nucleate boiling is indicated in Fig. 10c. Fig. 10d and e shows the nucleate boiling of the medium accompanied by intensive cooling of the probe. The end of nucleate boiling and start of convective cooling is shown in Fig. 10f. The bubble formation starts at the lower end and ascends to the top of the probe in both aqueous and oil media. In aqueous media like water and brine the formation, growth and departure of bubble would take place easily and require low superheat due to their low viscosity and low boiling point. Due to their high boiling points and viscosities, oil quenchants require more amount of heat for nucleation and growth of the bubble. After bubble inception, the superheated liquid layer is pushed outward and mixes with the bulk liquid. The space vacated by the bubble after departure was filled with liquid from the cold pool. The larger size of the bubble increases the amount of cold liquid to contact the interface of the probe resulting in higher rate of heat transfer. Among vegetable oils, sunflower, coconut and palm oils show higher heat flux transients. Evaporation of the liquid to form the bubble might be easier in these low viscosity oils leading to larger size of the bubble resulting in higher rate of heat transfer. The water and brine quenchants showed a sharp peak in the heat flux transient curve compared with oil quenchants. The occurrence of peak was followed by a sharp decrease in heat flux transients at the specimen/quenchant interface indicating negligible thermal gradients inside the specimen at the later stages of cooling.

A maximum heat flux of 846 kW/m^2 was obtained with 5% brine solution and the castor oil yielded the lowest peak heat flux value of 401 kW/m^2. Heat flux obtained during quenching in palm oil (577 kW/m^2) was higher than mineral oil (472 kW/m^2). End quenching results also showed that cooling rate was strongly dependent on viscosity of quenching oils. Oils with higher viscosity offers greater resistance to the motion of vapour bubbles during nucleate boiling stage and the supply of cold liquid to the heated surface is reduced. This results in lower peak heat flux transients during quenching of stainless steel probe in higher viscosity castor oil. The thinning of oil at higher temperatures offsets the effect of increase in temperature and thus maintaining peak heat transfer rates for a longer time. Peak heat transfer coefficients are estimated for all the quench media.

The viscosities of water and brine solution at 27 °C are 1×10^{-3} Pa s and 2×10^{-3} Pa s, respectively. The variation of viscosity of oil quenchants with temperature is shown in

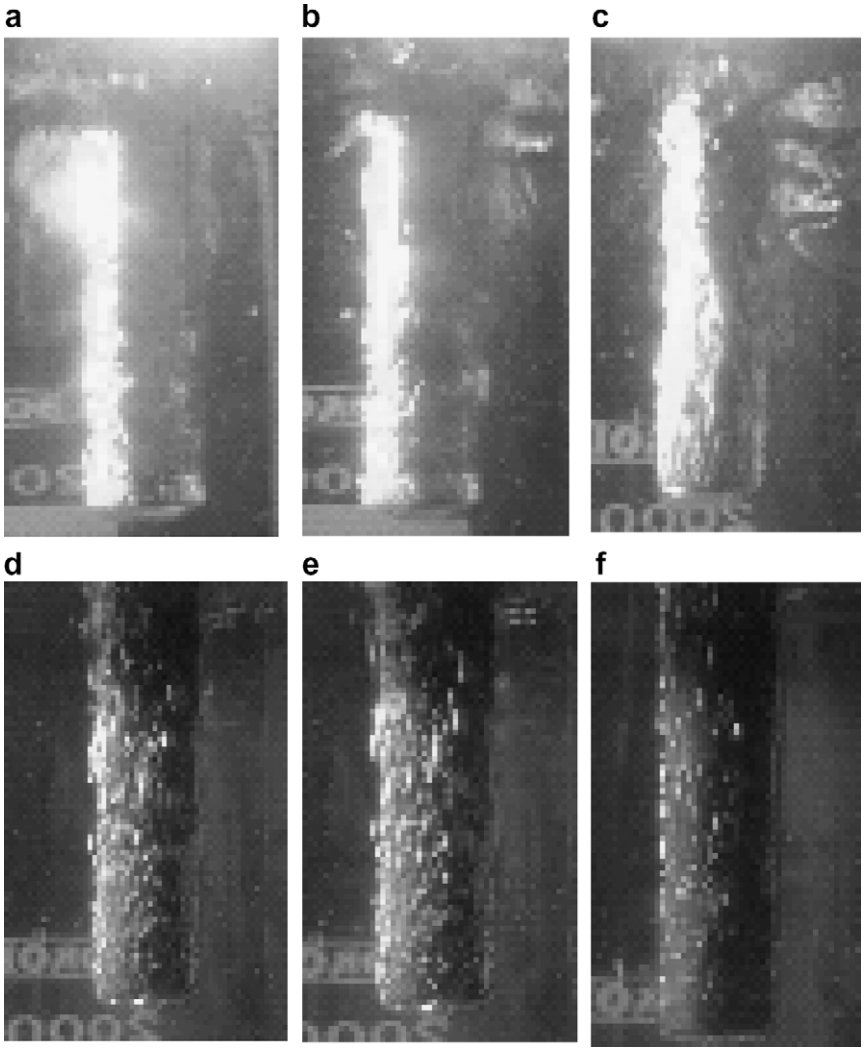

Fig. 10. Photographs of stainless steel probe during quenching in palm oil: (a)–(b) formation of vapour blanket, (c) end of vapour phase and start of nucleate boiling, (d)–(e) nucleate boiling and intensive cooling, and (f) end of nucleate boiling and start of convective cooling.

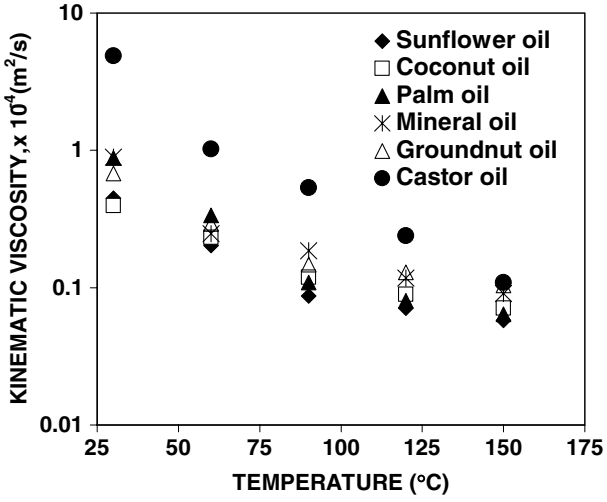

Fig. 11. Variation of viscosity of different oils with temperature.

Fig. 11. The viscosity of palm oil in the temperature range of 100–140 °C was significantly lower. Temperature of palm oil during end quenching was around 140 °C. Although the viscosity of palm oil is higher at lower temperature ($v_{30\,^\circ C} = 0.883 \times 10^{-4}$ m^2/s), its viscosity decreases significantly at higher temperatures ($v_{150\,^\circ C} = 0.064 \times 10^{-4}$ m^2/s) and this contributes to higher rates of heat transfer during quenching in palm oil. Further, all vegetable oils used in the present investigation have higher flash and fire points compared to the mineral oil as shown in Table 1.

A comparison of severity of quench assessed by cooling curve analysis with measured hardness during end quenching of AISI 1040 steel in various quench media is shown in Table 2. Brine quenched specimens showed higher hardness compared to that obtained with water quenched samples although the viscosity of brine is more than twice that of water. This is due to the existence of a stable vapour phase film during water quenching. During quenching with brine, it is likely that a localized increase in the concentration of the sodium chloride would occur near the specimen due to

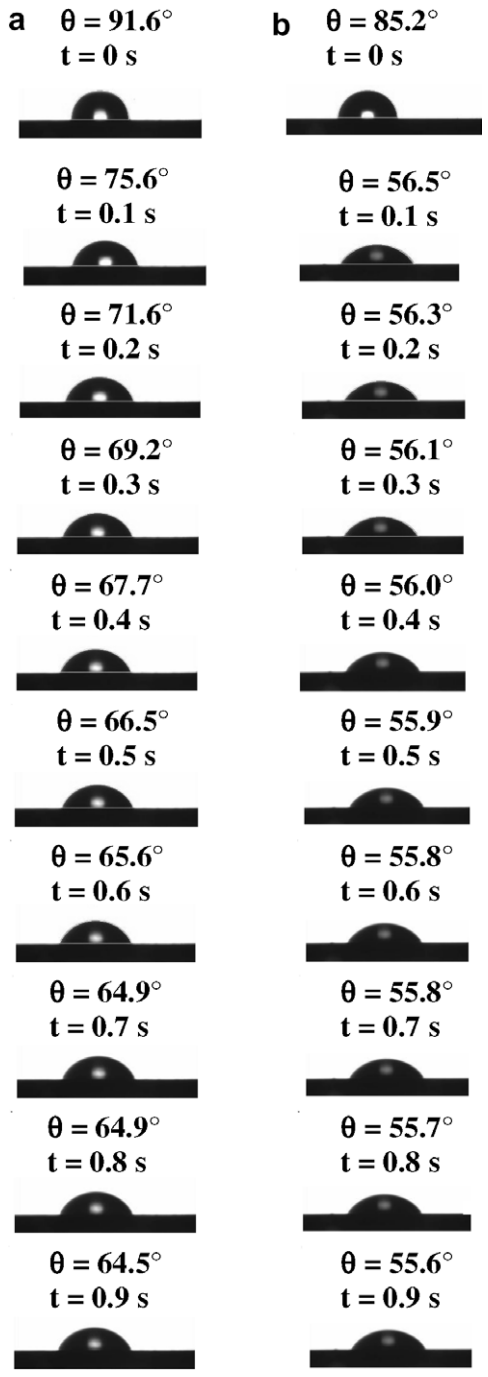

Fig. 12. Images showing contact angle relaxation of water on stainless steel substrate at (a) 30 °C and (b) 75 °C.

Table 1
Flash, fire and boiling points of oil quenchants

Quench oil	Flash point (°C)	Fire point (°C)	Boiling point (°C)
Sunflower	255	280	205
Coconut	258	304	200
Palm	300	335	255
Mineral (SN150)	230	260	172
Groundnut	312	340	260
Castor	285	315	245

Table 2
Comparison of quench severity and hardness of AISI 1040 steel during end quenching

Quench medium	Grossman quench severity (m^{-1})	Hardness (R_a)
Brine (5%)	47	63
Water	38.5	62
Sun flower oil	21.6	53
Coconut oil	21.6	53
Palm oil	20.8	51
Mineral oil	18.4	50
Groundnut oil	16.1	47
Castor oil	12	47

Table 3
Heat transfer coefficients estimated by different techniques

Quench medium	Estimated heat transfer coefficient, h (W/m^2 K)		
	Grossman's method	Kobasko's method	Inverse analysis – end quench
5% Brine	2258	1255	1516
Water	1848	1100	1480
Sunflower oil	1037	721	1158
Coconut oil	1037	708	1082
Palm oil	998	691	1072
Mineral oil	884	672	841
Groundnut oil	774	600	802
Castor oil	567	528	764

the evaporation of water. This could result in the destabilization of the insulating vapour blanket increasing the rate of heat transfer from the specimen to the quench medium. It is interesting to note that the castor oil with the lowest severity of quenching yielded specimens having lower values of hardness compared to that obtained with other quench media.

Quench severity of aqueous and oil media used in the present investigation are arranged in the following order:

$$\text{Brine} > \text{Water} > \text{Sunflower oil} > \text{Coconut oil} > \text{Palm oil} > \text{Mineral oil} > \text{Groundnut oil} > \text{Castor oil}$$

The severity of quenching of sunflower, coconut and palm oils was higher compared to mineral oil. These vegetable oils could be used as quench media for industrial heat treatment. Table 3 gives the heat transfer coefficients estimated by the three different techniques adopted in the present work. The heat transfer coefficients estimated by Grossman's technique ($\bar{h}$) and the inverse analysis (h_{max}) are higher as compared to the Kobasko's technique (h_{max}). However, the variation of heat transfer coefficients for different oils is similar. For example, a lowest heat transfer coefficient was obtained for castor oils in all the three techniques.

4.1.4. Wetting behaviour

Figs. 12 and 13 show the images of sessile drops of water and castor oil at various temperatures, respectively. Fig. 14 shows the relaxation of various quench media on a stainless

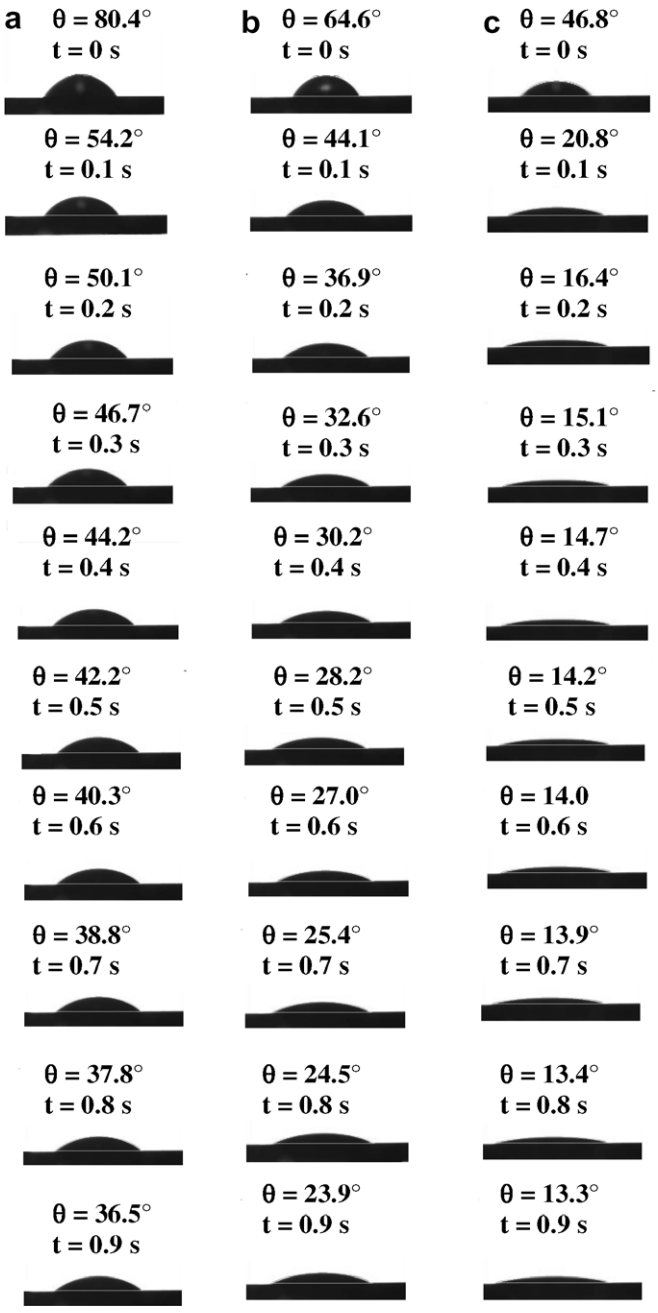

Fig. 13. Images showing contact angle relaxation of castor oil on stainless steel substrate at (a) 30 °C, (b) 75 °C and (c) 175 °C.

steel plate at 30 °C. The relaxation of contact angle was rapid during early stages and it became gradual as the system approached equilibrium. Higher contact angles were obtained for water. The change of contact angle during relaxation was low for water indicating low spreading. However, contact angles significantly decreased during spreading of oil media. It shows that the equilibrium contact angle decreases with increase in the temperature of the substrate.

Fig. 15 shows the temperature dependency of spreading of quench media. The time required to reach the equilibrium state decreases with increase in temperature. Less time

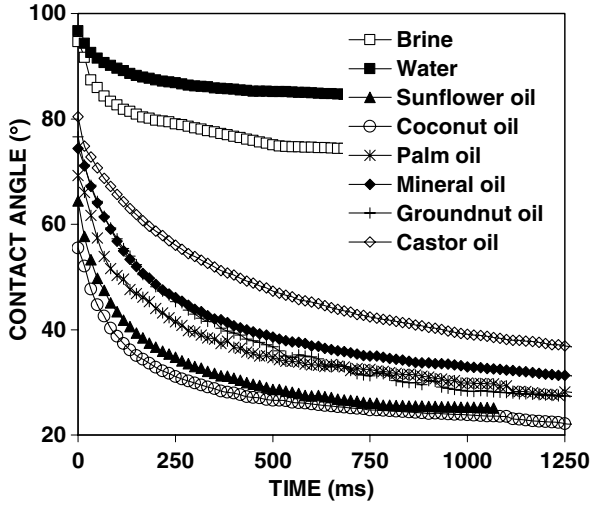

Fig. 14. Relaxation of contact angles of different liquids on stainless steel substrate ($R_a = 0.75$ μm) at 30 °C.

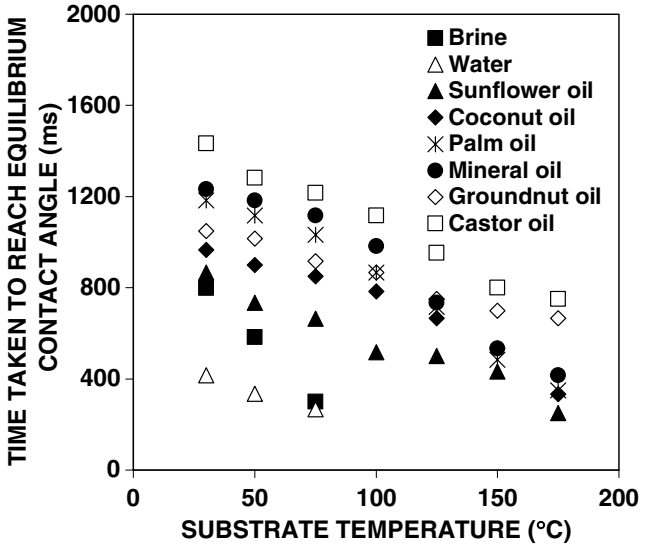

Fig. 15. Temperature dependency of equilibrium contact angle for spreading of liquid media.

was required to reach the equilibrium state for aqueous media as compared to oil media. The time taken to reach the equilibrium contact angle for brine at different temperatures of the stainless steel substrate was more as compared to water. For example, the time taken to reach equilibrium contact angle for brine was 799 ms and for water was 416 ms at 30 °C. This indicated that spreading of brine was more than water on stainless steel substrate. Highest relaxation time (1433 ms at 30 °C) was obtained for castor oil to reach equilibrium state and lowest time (866 ms at 30 °C) was obtained for sunflower oil. Mineral oil showed an intermediate value (1233 ms at 30 °C). The relaxation time decreased to 750, 250, 417 ms for castor, sunflower and mineral oils on stainless steel substrate at 175 °C, respectively.

Figs. 16 and 17 show the typical plots of spread area vs time for brine and castor, respectively. The spreading was significant for all quench media at higher temperatures. Low spreading was observed in aqueous media as compared to oil media. Higher spread area is the indication of the spreading of liquid drop during relaxation resulting in lower contact angle. Oils started spreading rapidly with a relatively high spread velocity resulting in a sharp increase of the base area during early stages of spreading. However, within a very short period the spreading rate significantly reduced to almost zero indicating the condition of stabilization. This is due to the attainment of equilibrium between the various surface forces under action.

The spreading behaviour of various oils on stainless steel substrate at different temperatures consisted of three stages, namely, capillary, gravity and viscous regimes. Capillary action is the dominating factor during initial stages of the spreading of liquid and this initial stage is called as capillary regime. Capillary action is the ability of a substance to draw a liquid against the force of gravity. It occurs when the adhesive intermolecular forces between the liquid and a solid are stronger than the cohesive intermolecular forces within the liquid. Gravitational force is the deciding factor in gravity regime. Viscous force is the dominating force, to cease the flow of liquid due to intermolecular resistance in viscous regime. Fig. 18 shows the effect of temperature on spreading of sunflower oil. The spreading begins with an initial capillary regime followed by a gravity regime and ends in viscous regime. At lower temperature (30 °C) the spreading was still in the gravity regime with nearly a constant slope which indicates that the spreading of the oil has not been terminated. However, at higher temperature (175 °C), sunflower oil spreading was almost terminated and this was indicated by the existence of viscous regime.

Fig. 19 shows the effect of temperature on the spreading of sunflower, palm and castor oils. A similar behaviour was

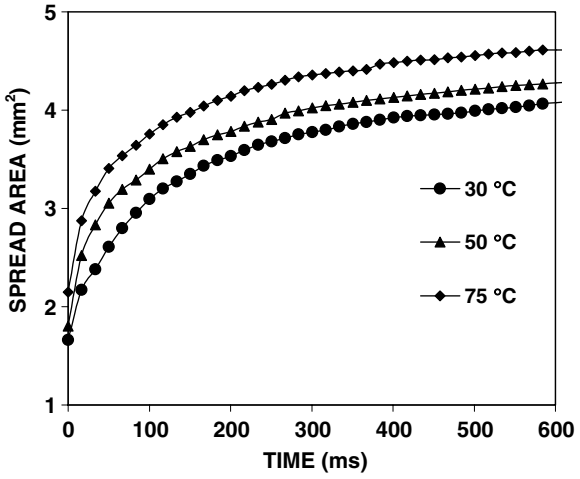

Fig. 16. Variation of spread area with time during spreading of 5% brine on stainless steel substrate.

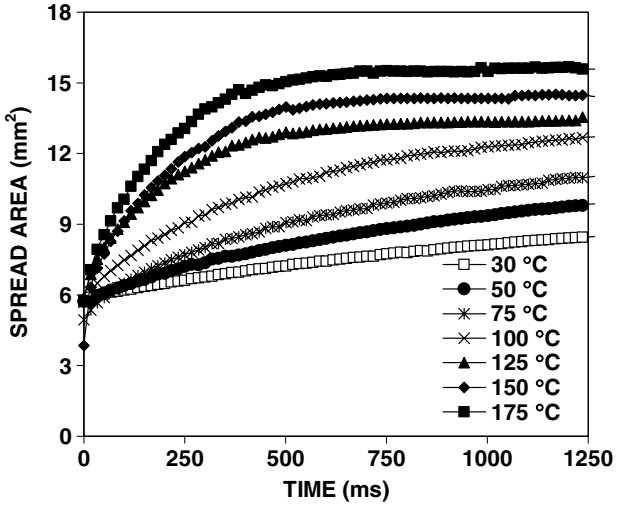

Fig. 17. Variation of spread area with time during spreading of castor oil on stainless steel substrate.

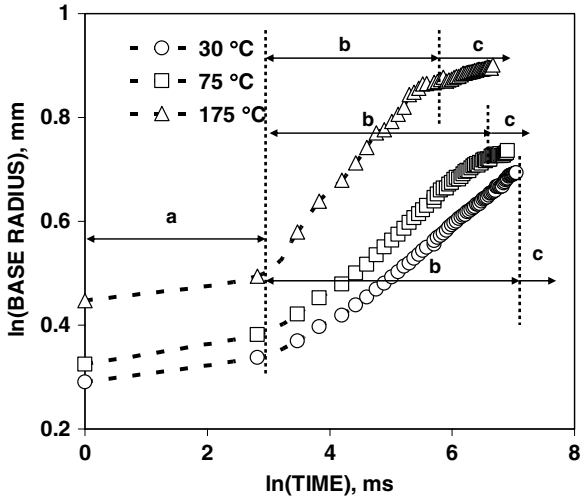

Fig. 18. Effect of temperature on spreading of sunflower oil on stainless steel substrate showing (a) capillary, (b) gravity and (c) viscous regimes.

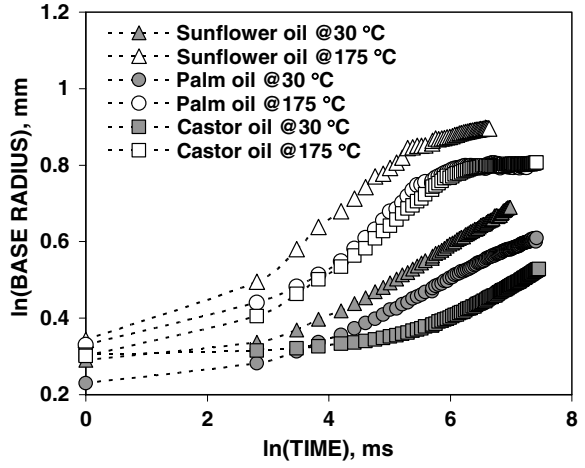

Fig. 19. Effect of substrate temperature on spreading regimes for various oils.

observed during spreading of other quench oils as well at different temperatures. A comparison of the spreading behaviour at various temperatures indicated the significant difference between lower viscosity and higher viscosity oils. The increase in temperature of the substrate accelerates the spreading of oil medium. The increase in temperature reduces the viscosity of the liquid resulting in the increase of the ease of spreading. Among oils, lower viscosity oils like sunflower and coconut oils show higher base radius as compared to higher viscosity castor oil. Higher viscosity oil offers greater resistance to flow as compared to lower viscosity oil resulting in lower contact area as shown in the spreading of castor oil. Conventional mineral oil (SN150) exhibited the intermediate spreading behaviour.

4.1.5. Dimensionless contact angle parameter

The severity of quenching of aqueous media was greater than oil media although their wettability was poor as indicated by their higher contact angles. It is not possible to relate the wetting behaviour of both aqueous and oil quench media with the rate of heat transfer from the probe to the quench medium. Hence two dimensionless parameters ϕ and τ are defined to represent contact angle and time variables, respectively, in order to carryout at a meaningful comparison of wetting behaviour with heat transfer for both aqueous and oil quench media. The dimensionless contact angle relates the degree of wetting (contact angle) with the rate of wetting (spreading) of quench media. The dimensionless contact angle (ϕ) is defined as $\phi = (\theta - \theta_r)/(\theta_i - \theta_r)$. The reference contact angle (θ_r) is defined as the value of θ beyond which $d\theta/dt$ is $\leqslant 0.01$ °/ms. Dimensionless time (τ) is defined as $\tau = (t/t_r)$. t_r is the time taken for the drop to evolve from θ_i to θ_r on a substrate and t is the transient time. Figs. 20 and 21 show the variation of dimensionless contact angle with dimensionless time of various quench media on a stainless steel substrate at 30 °C and 75 °C, respectively. The analysis revealed that the

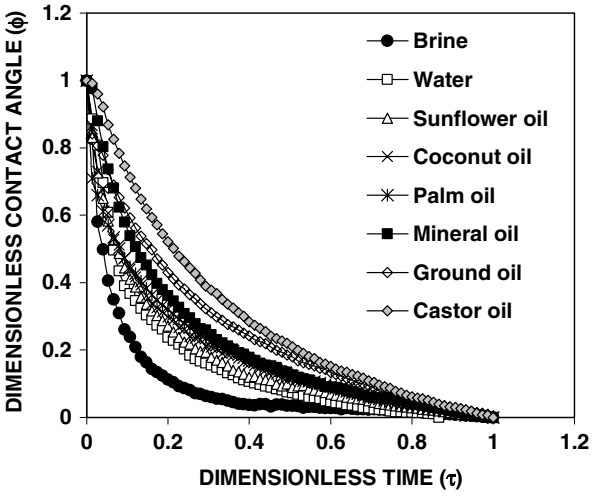

Fig. 20. Relaxation of dimensionless contact angles of quench media on stainless steel substrate at 30 °C.

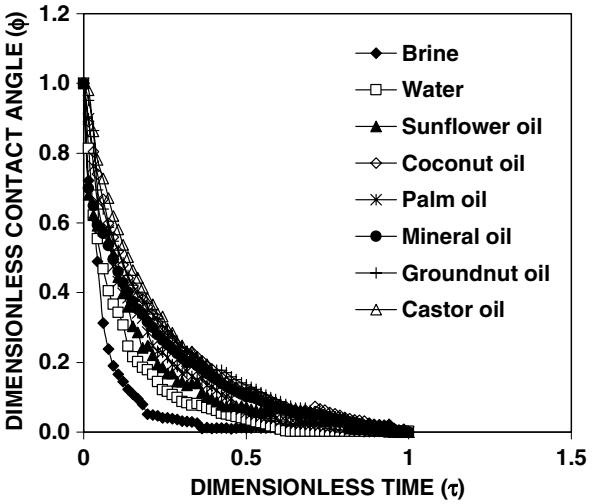

Fig. 21. Relaxation of dimensionless contact angles of quench media on stainless steel substrate at 75 °C.

relaxation of dimensionless contact angle for aqueous media was faster compared to oil media although the absolute values of contact angles of aqueous media were higher. Among oil quenchants, the sunflower oil showed a sharp decrease in the dynamic dimensionless contact angle as compared to other oils. The results of wetting behaviour and heat transfer analysis were found to be in good agreement. The wetting characteristics and quench severities of palm oil and mineral oil were comparable. However it is important to assess and compare the thermal stability of palm oil with mineral oil.

4.1.6. Thermal stability of oil quench media

The thermal stability of oil is defined as the resistance to thermal degradation and it was determined by finding the total acid number (TAN) and iodine number (IN). Total acid number (TAN) is defined as the amount of potassium hydroxide (in mg) necessary to neutralize the free fatty acids in 1 g of oil sample [12]. Iodine number of oil is amount of iodine (in g) absorbed by 100 g of oil or fat. The TAN value of the oil is an indication of the level of oxidation. Oxidation of the quench oil takes place due to repeated heating and cooling. Iodine number measures the level of unsaturated fats and oils. The TAN of both palm oil and mineral oil increased with ageing. However iodine numbers of both oils decrease with increase in the number of quench cycles. The effect of ageing on TAN and IN of both palm and mineral oils are shown in Figs. 22 and 23, respectively. The total acid number of mineral oil is considerably higher at about 15.6 mg of KOH/g after about 200 thermal cycles. The corresponding TAN of palm oil is only 8.7 mg of KOH/g. A similar trend was observed for variation in the iodine number (IN) with thermal cycling. The rate of change of TAN and IN of palm oil on thermal cycling was negligible as compared to the mineral oil. The dynamic contact angle increased on thermal ageing of both palm and mineral oils as shown in

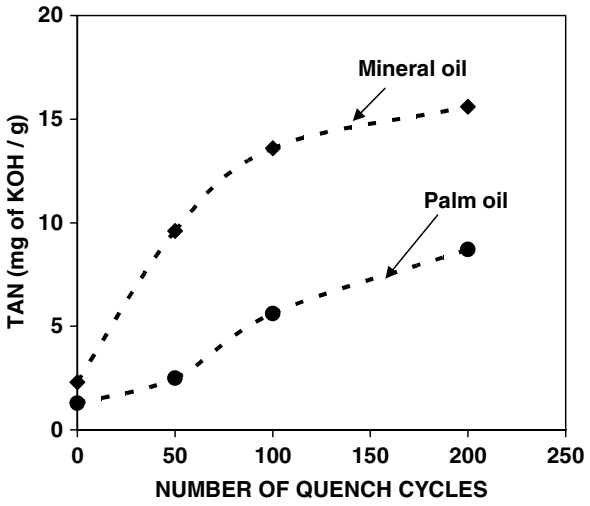

Fig. 22. Effect of ageing on total acid number of mineral and palm oils.

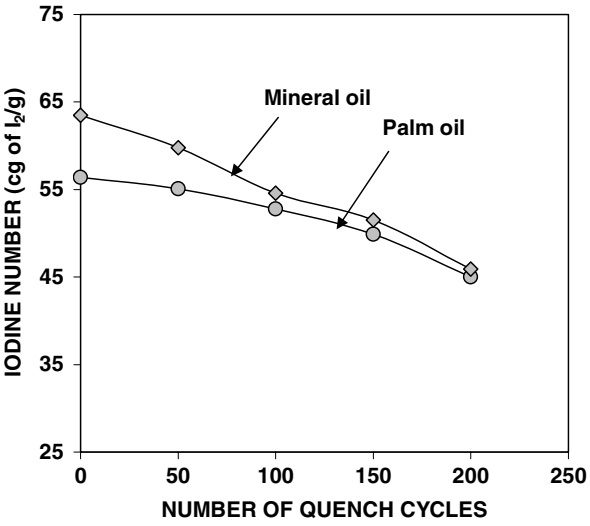

Fig. 23. Effect of ageing on iodine number of mineral and palm oils.

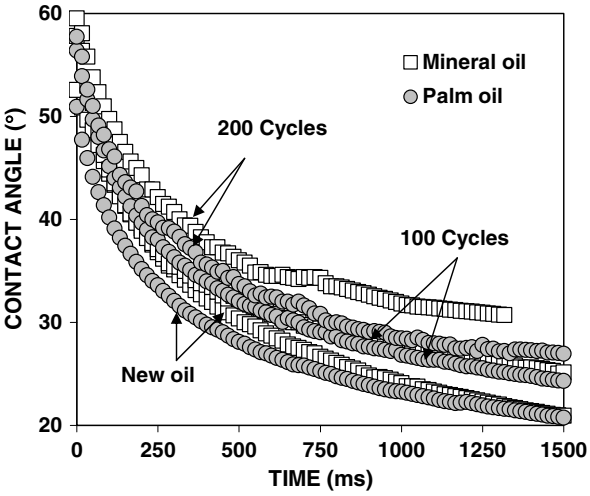

Fig. 24. Effect of ageing on contact angles of mineral and palm oils.

Fig. 24. It was also observed that dynamic contact angles of palm oil were lower than mineral oil. The results show that the thermal stability of palm oil is better than mineral oil. Palm oil is thus safer compared to mineral oil and its thermal stability is superior to mineral oil. Thus palm oil could be exploited as an effective bioquenchant for industrial heat treatment.

5. Conclusions

1. Grossman quench severity factor (H) is an effective tool to assess the severity of quenching of aqueous and oil media. However it cannot distinguish various bioquenchants having only a slight difference in the severity of quenching among them. Inverse analysis is more suitable for the assessment of quench severity of bioquenchants.
2. Among vegetable oils, highest heat transfer coefficients were obtained for sunflower oil and lowest heat transfer coefficients were obtained for castor oil.
3. The heat flux during quenching was found to be strongly influenced by the viscosity of quench media. Oils with higher viscosity resulted in reduced cooling rates.
4. Based on the heat flow parameters, the quench severities of various bioquenchants and mineral oil are arranged in the following order:

$$\text{Sunflower oil} > \text{Coconut oil} > \text{Palm oil} > \text{Mineral oil} > \text{Groundnut oil} > \text{Castor oil}$$

5. A higher degree of spreading was observed in oil media as compared to aqueous media. The time required for relaxation of droplet of quench medium decreased with increase in temperature of the substrate.
6. Although the wettability of aqueous quench media is poor, their severity of quenching is greater than oil media. For oils, higher rate of heat transfer was associated with higher wettability of the medium. Dimensionless contact angle $[\phi = (\theta - \theta_r)/(\theta_i - \theta_r)]$ defined in the present work was found to be a better parameter to compare the wetting behaviour of aqueous as well as oil quench media with the severity of quenching.
7. Total acid number (TAN) increased and iodine number (IN) decreased on thermal cycling of quench oils. The change in total acid number and iodine number on thermal cycling was negligible in palm oil as compared to mineral oil. The thermal stability of palm oil is thus superior to mineral oil.

Acknowledgements

The excellent laboratory facilities offered at the Castings Research Centre (CRC) of the Department of Metallurgical and Materials Engineering, National Institute of Technology Karnataka is gratefully acknowledged. One of the authors (K.N.P.) thanks the Defence Research Development Organization (DRDO), Government of India, New

Delhi for providing financial assistance to purchase FTA 200 Dynamic Contact Angle Analyzer.

References

[1] G.E. Totten, Y. Sun, G.M. Webster, L.M. Jarvis, C.E. Bates, Quenchant selection, in: Proceedings of the 18th Conference of Heat Treating Symposium Including the Lui Dai Memorial Symposium, ASM International, Materials Park, OH, 1998, pp. 183–189.

[2] B. Liscic, State of the art in quenching, in: Proceedings of the Third Seminar of the International Federation of Heat Treatment and Surface Engineering, The Institute of Materials, London, 1993, pp. 1–32.

[3] D.L. Moore, S. Crawly, Applications of standard quenchant cooling curve analysis, in: Second ASM. Heat Treating and Surface Engineering Conference, Germany, 1993.

[4] R.A. Wallis, S. Owens, R.I. San Pedro, Four years experience using an inconel probe to test the cooling characteristics of production quench oil, in: Seventeenth ASM Heat Treating Society Conference Proceedings Including First International Induction Heat Treating Symposium, 1997, pp. 457–466.

[5] J. Bodin, S. Segerberg, Measurement and evaluation of the quenching power of quenching media for hardening, in: Proceedings of the Third Seminar of the International Federation of Heat Treatment and Surface Engineering, The Institute of Materials, London, 1993, pp. 33–54.

[6] S.J. Gokhale, J.L. Plawsky, P.C. Wayner Jr., Experimental investigation of contact angle, curvature and contact line motion in dropwise condensation and evaporation, J. Colloid Interface Sci. 259 (2003) 354–366.

[7] C.W. Extrand, Spontaneous spreading of viscous liquid drops, J. Colloid Interface Sci. 157 (1993) 72–76.

[8] S. Sikalo, C. Tropea, E.N. Ganic, Dynamic wetting angle of a spreading droplet, Exp. Therm. Fluid Sci. 29 (2005) 795–802.

[9] S.G. Kandlikar, M.E. Sterinke, Contact angles and interface behaviour during rapid evaporation of liquid on a heated surface, Int. J. Heat Mass Transfer 45 (2002) 3771–3780.

[10] T.D. Blake, Y.D. Shikhmurzaev, Dynamic wetting by liquids of different viscosity, J. Colloid Interface Sci. 253 (2002) 196–202.

[11] D.S. MacKenzie, L. Gunsalus, I. Lazerav, Effect of contamination on the cooling rate of quench oils, in: International Federation of Heat Treatment and Surface Engineering Conference, Croatia, 2001.

[12] W.B. Wan Nik, F.N. Ani, H.H. Masjuki, Thermal stability evaluation of palm oil as energy transport media, Energy Convers. Manage. 46 (2005) 2198–2215.

[13] N.I. Kobasko, G.E. Totten, G.M. Webster, C.E. Bates, Comparison of cooling capacity of aqueous poly(alkylene glycol) quenchants with water and oil, in: Proceedings of the 18th Conference of Heat Treating Symposium Including the Lui Dai Memorial Symposium, ASM International, Materials Park, OH, 1998, pp. 559–567.

[14] H.K. Kim, S.I. Oh, Evaluation of heat transfer coefficient during heat treatment by inverse analysis, J. Mater. Process. Technol. 112 (2001) 157–165.

[15] K.N. Prabhu, Investigation of heat transfer at the casting/die wall interface during solidification of aluminium base alloys, Ph.D. Thesis, Mangalore University, 1990.

[16] M. Raynaud, J.V. Beck, Methodology for comparison of inverse heat conduction methods, Trans. ASME 110 (1998) 30–37.

[17] A. Buczek, T. Telejko, Inverse determination of boundary conditions during boiling water heat transfer in quenching operation, J. Mater. Process. Technol. 155–156 (2004) 1324–1329.

[18] J. Hammad, Y. Mitsutake, M. Monde, Movement of maximum heat flux and wetting front during quenching of hot cylindrical block, Int. J. Therm. Sci. 43 (2004) 743–752.

[19] J.V. Beck, Nonlinear estimation applied to the nonlinear inverse heat conduction problem, Int. J. Heat Mass Transfer 13 (1970) 703–716.

[20] K.N. Prabhu, A.A. Ashish, Inverse modelling of heat transfer with application to solidification and quenching, J. Mater. Manuf. Processes 17 (2002) 469–481.

[21] V.K. Dhir, Review – Nucleate and transition boiling heat transfer under pool and external flow conditions, Int. J. Heat Fluid Flow 12 (1991) 290–313.